# Metabolic regulation of differentiation and maturation: from induced pluripotent stem cell to endothelial cell

Es - Tiemeier, G.L. van

Chapter 4

# PPARγ co-activator-1α (PGC-1α) - independent free fatty acid oxidation drives human iPSC-derived endothelial cell energy metabolism



This Thesis (in preparation for submission)

Gesa L. Tiemeier, Rosalie G.J. Rietjens, Gangqi Wang, Sarantos Kostidis, Wendy M.P.J. Sol, Sébastien J. Dumas, Martin Giera, Cathelijne W. van den Berg, Peter Carmeliet, Bernard M. van den Berg, Ton J. Rabelink

## Abstract

To meet the full potential of human induced pluripotent stem cells (hiPSC) and enable their applications in regenerative medicine, development of functional vasculature is a prerequisite. Previous studies have shown essential limitations in the maturation of hiPSC-derived endothelial cells (hiPSC-EC) coupled to altered cellular metabolism. In particular, hiPSC-EC have reduced glycolysis and reduced glucose flux to the tricarboxylic acid cycle (TCA) cycle. Nevertheless, hiPSC-ECs have retained their capacity for energy production in association with their proliferative capacity. Here we investigate whether free fatty acid (FFA) metabolism serves as the main metabolic energy pathway in hiPSC-EC. When compared to microvascular endothelium, hiPSC-EC have a significantly higher FFA dependent mitochondrial respiration. hiPSC-ECs use free fatty acids as a potent alternative acetyl-CoA source to generate ATP and for regeneration of NADPH from $NADP^+$, in order to maintain the redox balance of the cell. In line with the reliance on FFA oxidation we found increased amounts of lipid droplets for storage of fatty acid in iPSC-EC. Interestingly, the transcriptional co-activator peroxisome proliferator-activated receptor gamma co-activator 1 alpha (PGC-1α), absent in primary EC such as human microvascular endothelial cells (hMVECs) and human umblical vein cells (HUVECs), was significantly upregulated in hiPSC-ECs. PGC-1α is known to be the master regulator of energy homeostasis; affecting glucose uptake, FFA uptake/storage and oxidation as well as mitochondrial biogenesis. PGC-1α knockdown in hiPSC-EC, however, did not result in the expected reduction of fatty acid-driven mitochondrial respiration or induction of glucose driven metabolism. We therefore conclude that hiPSC-EC use FFA for the production of energy, maintaining the redox balance and produce precursors of biosynthesis, independent of PGC1 α regulation.




## Introduction

In the last decades, the interest in regenerative medicine has significantly increased within the field of biomedical research.[1-4] Tissue regeneration has the potential not only to be used as an *in vitro* research technique but also to be implemented as a tool for disease modeling and therapeutics.[3] Its potential as a treatment especially became feasible upon the discovery of induced pluripotency of mature human cells.[5,6,7] Creating hiPSCs was initially achieved by introducing four genetic factors: *OCT3/4, SOX2, KLF4* and *c-MYC*.[5,8,9] A prerequisite for realizing the potential of human induced pluripotent stem cells (hiPSCs) in regenerative medicine is the generation of a functional vasculature in the organoid of interest.



The most important layer of the vasculature are the cells that form the inner layer, the endothelial cells (EC). One key aspect of functional endothelial cells is their metabolism, as this is responsible for production of energy, generation of catabolic substrates and signaling molecules as well as maintenance of the redox balance.[10,11] EC metabolism has only been a research interest during the last few years.[12] This research shows that in embryonic development, stem cells first need to make a switch towards the more oxidative phosphorylation (OXPHOS) dependent mesoderm lineage, after which differentiation to ECs requires a switch back to glycolysis. Under normal conditions, ECs rely greatly on glycolysis without maximizing energy production by OXPHOS, presumably to minimize oxidative stress in an oxygen-rich environment.[13] During angiogenesis, the formation of new blood vessels from pre-existing vessels, ECs upregulate glycolysis even more to drive this process.[14] On the other hand, quiescent ECs switch to a higher fatty acid β-oxidation (FAO) to maintain redox balance.[15] This continuous switching requires great plasticity in the metabolic pathways of the cell.

Furthermore, primary cells in the human body also have their own distinct metabolic fingerprint dependent on their function and cellular state.[16] It also means that after differentiation the metabolic profile of the differentiated hiPSCs should be compared to their primary cell counterpart to assess their phenotypical comparability in functional assays or *in vivo* applications.

Thus far, hiPSC-EC metabolism has not been studied extensively despite its importance in functionality of such differentiated cells. In the current study, we compared hiPSC-EC metabolism to primary human microvascular endothelial cells (hMVEC). To this end we examined the differences in two important metabolic pathways, the glucose and fatty acid oxidation. We investigated the transcriptional

coactivator peroxisome proliferator activated receptor gamma coactivator 1 alpha (PGC-1α) as a target for improving the metabolic state of hiPSC-ECs necessary for proper endothelial function.

## Materials and methods

### hiPSC-EC differentiation

For human hiPSC-EC differentiation, the NCRM1 hiPSC line was used and differentiated according to Orlova et al.[17] (kindly provided by prof. dr. Mummery, dept. of Anatomy and Embryology, LUMC, Leiden, the Netherlands).

Human iPSCs were cultured on Matrigel coated plates in mTeSR1 PSC/E8 medium (Stem Cell technologies) and were enzymatically passaged once per week using the same routine. Differentiation was induced 4 days after passaging (day 0). Mesoderm specification was induced by adding bone morphogenetic protein 4 (BMP4), activin A, small-molecule inhibitor of glycogen synthase kinase-3β (CHIR) and vascular endothelial growth factor (VEGF). These factors were removed on day 3 and were then replaced with vascular specification medium supplemented with VEGF and transforming growth factor-β (TGF-β) pathway small-molecule inhibitor SB431542. This inhibitor specifically affects activin receptor-like kinase-4, activin receptor-like kinase-5 and activin receptor-like kinase-7 type I receptors (ALK-4, ALK-5 and ALK-7 respectively). Furthermore, it supports the expansion of ECs by inhibiting the antiproliferative activities of the present cell-derived TGF-β-like factors. On days 7 and 9 of differentiation this vascular specification medium was also refreshed, and on day 10 the ECs were isolated. This isolation was done using immunomagnetic selection with anti-CD31 antibody-coupled magnetic beads (Dynabeads®, Miltenyi Biotech B.V., Leiden, the Netherlands). After isolation, ECs were transferred to EC serum free medium (EC-SFM) (Gibco, ThermoFisher Scientific, Waltham, MA) with added platelet-poor plasma serum (1% vol/vol) (Biomedical Technologies Inc. Stoughton, MA), 50 µg/ml VEGF-165 (R&D Systems), 100 µg/ml basic fibroblast growth factor (bFGF) (Miltenyi Biotech) and antibiotics (100 IU/ml penicillin and 100 µg/ml streptomycin).

### hMVEC

Primary human glomerular derived microvascular ECs (hMVECs) are isolated from human kidney cortical tissue and were purchased from Cell Systems (ACBRI-128, Kirkland, WA). They were available at passage 3 (< 12 cumulative population doubling) cryopreserved in CSC Cell Freezing Medium (4Z0-705). hMVECs were cultured in Endothelial Cell Growth Medium 2 (EGM2, PromoCell, Heidelberg, Germany) supplemented with antibiotics (100 IU/ml penicillin and 100 µg/ml streptomycin) and the Growth Medium 2 Supplement Pack (PromoCell). This supplementation leads to the following final concentration of the additives: Fetal Calf Serum (0.02 ml/ml), Epidermal Growth Factor (5 ng/ml), bFGF (10 ng/ml), insulin-like growth factor (Long R3 IGF, 20 ng/ml), VEGF (0.5 ng/ml), ascorbic acid (1 µg/ml), heparin (22.5 µg/ml) and hydrocortisone (0.2 µg/ml). Cells were always passaged once after thawing before performing experiments.

### Primary antibodies

Antibodies used to detect PGC-1α were obtained from both Novus Biologicals (NBP1-04676) and Invitrogen (PA5-38022). The antibody used for GAPDH detection was that from Cell Signaling Technologies (GAPDH (D16H11) XP® Rabbit mAb #5174). For MCT1, the MCT1 Antibody (20139-1-AP) from Proteintech was used.

### Western blotting

After experimental procedures, hiPSC-ECs and hMVECs were lysed in lysis buffer (50 mM Tris-HCl, 150 mM NaCl, 1% SDS deoxycholate, 0.5% Triton X-100) supplemented with Pierce™ Protease and Phosphatase Inhibitor (ThermoFisher Scientific). Sonication was used on these lysis samples to achieve complete cell disruption. Protein concentration of the samples was determined using the Pierce™ BCA Protein Assay Kit (ThermoFisher Scientific). Samples for Western blotting were prepared using 6.5 µg protein, Red Loading Buffer Pack (1:4, NEB, MA, United States), dithiothreitol (DTT, 1:10, Bio-Rad Laboratories Inc, Ca, United States) and lysis buffer supplemented with protease inhibitor. The prepared samples were incubated at 95°C for 10 minutes and subsequently loaded on a Mini-PROTEAN® TGX™ Precast Gel (Bio-Rad). After electrophoresis, proteins were transferred on a PVDF (Bio-Rad) and detected with antibodies against PGC-1α (Invitrogen 1:1000, Novus Biologicals 1:500), MCT1 (1:5000) and GAPDH (1:600). After incubation, the membrane was incubated with a HRP-conjugated antibody (1:5000, Dako P0448) at RT for 1 hour. Signal was subsequently generated with Western Lightning® Plus-ECL (PerkinElmer, Waltham, MA) and analyzed with a ChemiDoc™ Imaging System (Bio-Rad).

### Lentiviral vector production

To produce the lentiviral expression vectors, competent *E. coli* cells were transformed with the following plasmids, kindly provided by the Dept. of Cell & Chemical Biology: TRCN0000001165, TRCN0000001166, TRCN0000001167, TRCN0000001168 for PGC-1α. The used plasmid to produce a mock control was the MISSION® pLKO.1-puro Non-Mammalian shRNA Control Plasmid DNA (Merck). After scaling up the bacteria plasmid into a 1 L Erlenmeyer flask, DNA was isolated from the bacteria using the

PureYield™ Plasmid Maxiprep System (Promega Corporation, Madison, WI). In order to produce the lentivirus, HEK293T cells were cultured in DMEM medium to a 40-60% confluent state. These cells were transfected with polyethylenimine (PEI) to introduce either the sPGC-1α or shMCT1 plasmid and two lentivirus plasmids, pVSVG and psPAX2. Cells were incubated overnight (37°C and 5% $CO_2$) after which medium was replaced with fresh DMEM for another 24 hours before collecting the virus-containing medium on the two consecutive days. The medium was filtered using a 0.45 um filter to make it ready to use for transduction.

## Lentiviral transductions

For transduction of hiPSC-EC with the lentiviral expression vector for the PGC-1α shRNA or mock, cells were cultured to a 50-70% confluent state in EC-SFM medium and transduced with the lentivirus together with 8 µg/ml polybrene (Merck). Cells were incubated overnight (37°C and 5% $CO_2$) after which the medium was replaced with fresh EC-SFM for another 24 hours before collecting them for experimental assays. The same protocol was used for the hMVECs and the shMCT1 lentiviral transduction, with the only difference that the medium used was the EGM2 medium.

## RNA isolation and qPCR

After experimental procedures, hiPSC-ECs and hMVECs were treated with TRIzol® Reagent (Invitrogen, Carlsbad, CA) and the samples were subsequently processed with the RNeasy Mini Kit (Qiagen, Hilden, Germany) to yield the RNA. Quantitative polymerase chain reaction (qPCR) was then performed using iQ SYBR Green Supermix on an iCycler real-time detection system (Bio-Rad). The used forward (FW) and reversed (RV) for the various genes are depicted in Table 1. The amplification volume was made up out of 6.5 µl iQ SYBR Green PCR master mix, 3 µl RNAse free water, 3 µl cDNA and 0.5 µl primers, resulting in a total volume of 13 µl. The Ct values of the examined gene were normalized with the Ct value of the housekeeping gene glyceraldehyde-3-phosphate dehydrogenase (GAPDH).

## RNA sequencing

After RNA isolation, RNA sequencing was done for three different cell lines, namely hMVECs, hiPSC-EC NCRM1 and hiPSC-EC L99. This was done in collaboration with the KU Leuven according to the protocol as described before.[47] The "DESeq2" R package was used to normalize the raw count and to perform the differentially expressed genes screening. Here, the hMVEC was set as the control to compared with hiPSC-EC NCRM1 and L99.



**Table 1. Gene sequence of primers used for qPCR**

| Gene | | Sequence |
|---|---|---|
| GAPDH | hu GAPDH fw | CACCCATGACGAACATGGG |
| | hu GAPDH rev | TTCCAGGAGCGAGATCCCT |
| ppargc1a | hu PGC-1α FW | AAACTTGCTAGCAGTCCTCA |
| | hu PGC-1α RV | TGGCTGGTGCCAGTAAGAG |
| PKM | Hu_PKM2_Fw | CCACTTGCAATTATTTGAGGAA |
| | Hu_PKM2_Rv | GTGAGCAGACCTGCCAGACT |
| Tfam | hu Tfam FW | ATGGCGTTTCTCCGAAGCAT |
| | hu Tfam RV | TCCGCCCTATAAGCATCTTGA |
| ppara | hu PPARA FW | ATGGTGGACACGGAAAGCC |
| | hu PPARA RV | CGATGGATTGCGAAATCTCTTGG |
| pparb | hu PPARB FW | GCCTCTATCGTCAACAAGGAC |
| | hu PPARB RV | GCAATGAATAGGGCCAGGTC |
| esrra | hu ESRRA FW | AGGGTTCCTCGGAGACAGAG |
| | hu ESRRA RV | TCACAGGATGCCACACCATAG |
| nrf1 | hu NRF1 FW | AGGAACACGGAGTGACCCAA |
| | hu NRF1 RV | TATGCTCGGTGTAAGTAGCCA |
| Notch1 | hu Notch1 FW | CGCTGACGGAGTACAAGTG |
| | hu Notch1 RV | GTAGGAGCCGACCTCGTTG |
| MCT1 | hu MCT1 fw | AGTAGTTATGGGAAGAGTCAGCA |
| | Hu MCT1 rev | GTCGGGCTACCATGTCAACA |

## Oil-red-O staining

A stock solution with Oil red O powder (Sigma-Aldrich C.I 26125) was prepared by dissolving 60 mg in 20 ml 100% 2-propanol, mixed well and left undisturbed for at least 20 minutes. This stock solution was stored at room temperature. The working solution was prepared freshly max 15min before use by diluting the stock solution with 3 parts stock and 2 parts distilled water. This was mixed well and left undisturbed for 10min followed by filtration through Whatman No. 1 filter paper.

Cells were cultured in ibidi 8-well slides as described before. After removing the supernatant from the Ibidi 8 well precoated culture slides, cells were washed once with phosphate-buffered saline (PBS) and fixed with 4% PFA + Triton X-100 (0,2%) in PBS for 2 min at room temperature. This first fixation step was removed, introducing a second fixation step of 45 minutes with Formalin 10% at room temperature (no washing was required in between the two steps). This was followed by washing the cells twice with distilled water to remove all fixatives and then incubating the cells

with a 60% 2-propanol solution for 5 minutes at room temperature. The Oil red O working solution was pipetted into the wells and to ensure a safely covering of the plate bottom, 0.2 ml per well was used for the 8-well slide. The cells were incubated at room temperature for 20 min with the Oil Red O working solution, followed by several washing steps with distilled water until the water was clear(approximately 5 times). Hereafter the Hematoxylin solution (undiluted) was applied for just 30 seconds and quickly removed by washing with distilled water . Finally the slides were then covered with water and imaged under light microscope (Lipid droplets appear red and nuclei appear blue).

## Transmission electron microscopy

Cell were grown in sterile cell culture dishes (PS, 35x10mm, with vents, Greiner Bio-One GmbH). Just before fixation, the medium was removed and 2.5% glutaraldehyde (Electron Microscopy Sciences)/2% paraformaldehyde (Electron Microscopy Sciences, EMS)/2mM CaCl2 (Merck) in 0.15M sodium-cacodylate (Sigma-Aldrich) buffered solution was applied gently on top of the cells. Fixation was for 2 hours at room temperature. Cells were then rinsed 2x with 2mM CaCl2 in 0.15 M sodium-cacodylate buffered solution, and post-fixed for 1 hour on ice with a mixture of 1% osmium tetroxide (EMS), 1.5% potassium ferrocyanide (Merck) and 2mM CaCl2 in 0.15 M sodium-cacodylate buffer. Samples were further rinsed 2x with 2 mM CaCl2 in 0.15M sodium-cacodylate buffer, dehydrated overnight in 70% ethanol, followed by 80% ethanol (10 min), 90% ethanol (10 min), and 100% ethanol absolute (2x 15 min; 1x30 min). The cells were then permeated with a mixture of epon LX-112 (Ladd Research) and propylene oxide (Electron Microscopy Sciences) (1:1) for 1 hour, followed by polymerization in pure epon.. Ultrathin sections (90 nm) were collected onto copper slot grids (Storck Veco) covered by Formvar film and a thin carbon layer, then stained with an aqueous solution of 7% uranyl acetate for 20 minutes, followed by Reynold's lead citrate for 10 minutes. Samples were analysed at an acceleration voltage of 120 kV using an FEI Tecnai 12 (BioTWIN) transmission electron microscope (Thermo Fisher Scientific), equipped with a 4k Eagle CCD camera (Thermo Fisher Scientific). Automated data acquisition and stitching software was used to record virtual slides of the cells (Faas et al., 2012). Images were captured at 11.000x magnification, with binning 2, corresponding to a 2 nm pixel size at the specimen level.

## Seahorse assay

To measure endothelial glycolytic function, mitochondrial respiration and free fatty acid oxidation, hiPSC-ECs and hMVECs were seeded overnight at 4 x $10^4$ cells/well on fibronectin (Merck) coated Seahorse XF96 Cell Culture Microplates (Agilent Technologies, Santa Clara, CA). The plate was incubated in Seahorse XF base medium (Agilent) at 37°C for 1 hour in a non-$CO_2$ incubator before measuring the extracellular flux in an XFe96 Analyzer (Agilent). Both the oxygen consumption rate (OCR) and extracellular acidification rate (ECAR) were measured over 4 min periods with 2 min mixing in each cycle, with five cycles in total. Inhibitors and activators were used at the following concentrations: 5 mM glucose, 1 mM palmitate, 0.5 mM carnitine, 5 µM oligomycin, 1 µM FCCP, 100 mM 2-DG, 1 µM rotenone, 1 µM antimycin A and 40 µM CPT1a inhibitor (Abcam, Cambridge, United Kingdom). Cellular protein content was determined after flux analysis using the Pierce™ BCA Protein Assay Kit (ThermoFisher Scientific). Data is represented as OCR or ECAR normalized to protein.



## Metabolites analysis

Quantitative analysis of intracellular and extracellular metabolites in in vitro EC cultures was performed using NMR spectroscopy as described in detail elsewhere [48,49]. Briefly, hMVECs and hiPSC-ECs in triplicates were washed with warm PBS (37°C) to remove the culture medium and quickly quenched with liquid nitrogen to arrest metabolism. The cells well subsequently scraped of the plates and extracted using a cold (-80°C) solution of methanol/chloroform/water, 8.1:0.9:1 (v/v/v). After leaving the samples on dry ice for at least 30 min, the extracts were centrifuged for 20 min at 18000 × g, at -4°C.

Prior to washing ECs with PBS, 0.2 mL of culture medium were collected from each sample and mixed with 0.4 mL of cold (-80 °C) 100% LC-grade methanol to extract extracellular metabolites. All samples were subsequently placed at -80°C for at least 30 min and centrifuged for 20 min at 18000 × g, at -4°C.

The supernatants from both cell extracts and culture medium extracts were collected and dried with nitrogen gas. NMR samples of extracts were prepared by dissolving the dried material with 0.22 ml of 0.15 M phosphate buffer (pH 7.4) in deuterated water containing 0.05 mM trimethylsilyl propionic-d4¬-sodium salt (TSP-d4) as internal standard for NMR referencing and quantification. An 1D 1H-NMR spectrum was collected for each sample on a 14.1 T (600 MHz for 1H) Bruker Avance II NMR, using the 1D-NOESY experiment with presaturation as implemented in the spectrometer library (Topspin v3.0, pulse sequence: noesygppr1d; Bruker Biospin, Ltd). All spectra were processed to correct the phase and baseline and imported in Chenomx NMR suite 8.4 (Chenomx NMR suite, v8.0, Edmonton, Canada) for quantification of metabolites. The protein bullet was dissolved in lysis buffer (150mM NaCl, 1% SDS, 0.5% deoxycholate and 0.5% triton X-100, pH 7.5) with sonification. The protein concentration was measured using PierceTM BCA protein assay kit (ThermoFisher) according to its manual. All concentrations were normalised to the

total protein mass of each sample.

For $^{13}C$ fractional enrichment analysis, triplicates of hMVECs and hiPSC-ECs were cultured in glucose-free medium, enriched by 5 mM U-$^{13}C$6-D-Glucose for 24 hours and processed as described above. Fractional enrichment was calculated as described elsewhere [49] by deconvoluting and quantifying the protons at 5.52, 5.60 and 5.62 ppm (from UDP-GlcNAc, UDP-Glc, and UDP-GlcA, respectively), the protons at 5.99-6.03 ppm (overlapped peaks from all 3 sugars) and the protons at 7.9 ppm (overlapped peaks from all 3 sugars).

**Table 2. Gene abbreviations**

| Gene abbreviation | Explanation |
|---|---|
| *ENO2* | Enolase 2 |
| *HK2* | Hexokinase 2 |
| *MPC1* | Mitochondrial pyruvate carrier 1 |
| *PFKFB3* | 6-Phosphofructo-2-Kinase/Fructose-2,6-Biphosphatase 3 |
| *PFKM* | Phofructokinase, muscle |
| *PFKP* | Phosphofructokinase |
| *PGM2* | Phosphoglucomutase 2 |
| *PKM* | Pyruvate kinase |
| *ACADS* | Acyl-CoA dehydrogenase |
| *ACAT1* | Acetyl-CoA Acetyltransferase 1 |
| *ACOX3* | Acyl-Coenzyme A oxidase 3 |
| *CPT1C* | Carnitine Palmitoyltransferase 1C |
| *CPT2* | Carnitine Palmitoyltransferase 2 |
| *ECHDC2* | Enoyl-CoA hydratase domain containing 2 |
| *HADH* | Hydroxyacyl-coenzyme A dehydrogenase |
| *PPARGC1A* | Peroxisome proliferator-activated receptor gamma coactivator 1-alpha |
| *TFAM* | transcription factor A, mitochondrial |
| *NOTCH1* | Notch homolog 1, translocation-associated |
| *PPARA* | Peroxisome Proliferator Activated Receptor Alpha |
| *PPARB* | Peroxisome Proliferator Activated Receptor Beta |
| *NRF1* | Nuclear Respiratory Factor 1 |
| *ESSRA* | Estrogen Related Receptor Alpha |



Uptake/release was calculated as: ((Cspent – Cblank)*V)/ protein, where Cspent is the concentration of metabolite in the culure medium (mmol/lt), Cblank the concentration in the cell-free medium (mmol/lt) and V (lt) the volume of culture medium in each petri dish.

### Statistical analysis

Results are presented as mean ± s.d. or ± s.e.m., where N defines the number of biological replicates. Differences between groups were assessed by non-paired 2-tailed Student's t test. Difference between groups was assessed by ANOVA. P values < 0.05 were considered statistically significant.



## Results

### hiPSC-ECs have elevated free fatty acid oxidation

Human hiPSC-ECs were generated by the protocol of Orlova et al. and are compared to primary hMVECs.[17] First the metabolic properties of the cells were characterized by performing functional measurements of the oxygen consumption rate (OCR). The OCR is an indicator of mitochondrial function as oxygen is mainly consumed in the electron transport chain of the mitochondria.[18] When comparing hiPSC-ECs with hMVECs differences in mitochondrial function were observed. With glucose as energy substrate, hiPSC-ECs showed a reduced basal and maximal mitochondrial respiration, a reduced ATP-linked respiration and mitochondrial reserve capacity (Figure 1a-e). When the substrate was changed from glucose to the free fatty acid palmitate, however, maximum mitochondrial respiration, ATP-linked respiration and mitochondrial reserve capacity were significantly enhanced in hiPSC-ECs compared to the reduced values in hMVECs (Figure 1f-j). These results indicate that hiPSC-ECs have a reduced ability to use the glycolytic metabolites as a source for mitochondrial respiration, and instead depend more on free fatty acid oxidation (FAO) to fuel the mitochondria compared to hMVECs.

We used nuclear magnetic resonance (NMR) spectroscopy to further determine the cellular release and uptake of metabolites of iPSC-ECs. Although iPSC-EC have a reduced glycolysis as described previously [19], we observed accumulation of intracellular pyruvate (Supplemental figure 1a). This suggests that hiPSC-EC OXPHOS is preferably run via other sources of Acetyl-CoA, such as FFAs. Using FAO, large amounts of ROS are produced which potentially damage the cell. However, one of the most evident differences among hMVEC and hiPSC-EC are the reduced glutathione (GSH) levels

(Supplemental figure 1b). This is in agreement with a reduction in intracellular glycine (precursor of GSH) and reduced uptake of extracellular cystine (Supplemental figure 1c, d). Cystine is converted to cysteine in the cytosol and then stored as glutathione tripeptide to act as ROS scavenger. This indicates that although the cell produces a lot of ROS as shown before, the main ROS scavenger is not increasingly produced. This could explain the reliance on FFA oxidation of hiPSC-EC, since FFA oxidation regulates the redox balance by the NADPH/NADP$^+$ ratio.

## Abundant lipid droplets in hiPSC-ECs

To provide the cell with enough fatty acids for the increased FAO hiPSC-ECs were found to have increased amounts of lipid droplets (LD) for fuel storage compared to hMVEC (Figure 2a-d). On average 12.4% of iPSC-EC (±1.20%) were positive for oil-red-o compared to 2.5% (±1.66%) of the primary EC (Figure 2c), in line with previous study, suggesting EC rarely store fatty acids in LD in physiological conditions.[20] Interestingly, the iPSC-EC possess many, on average 22 per cell, very small LD (range 0.13µm -0,83 µm). On contrary, for example adipocytes have much larger LD, varying up to 100µm in size[21,22]. In specific situations, such as in high fat condition, LD formation in EC has at least three clear functions: to prevent lipotoxicity, provide FA to reduce glycolytic flux and for the release of FA from EC to adjacent cell types. On exposure to excessive amounts of FA, cells can esterify FA into TG-rich LDs via the Kennedy pathway to prevent lipotoxicity to the ER. LDs directly influence other metabolic processes in the cell, since LD lipolysis can attenuate glycolysis and impact glycolytic reserve in EC[23]. Peroxisome proliferator activated receptor gamma (PPAR-γ)4 has been reported to regulate FA uptake and transport in EC[24].

## Transcriptional co-activator PGC-1α is upregulated in hiPSC-ECs

The observed differences in metabolic characteristics initiated a more careful examination of the relevant metabolic pathways (Figure 3a). Analysis of RNA sequencing data of hiPSC-EC and hMVEC revealed that for glycolysis; *ENO2, HK2, MPC1, PFKFB3, PFKM, PFKP, PGM2, PKM* and for FAO; *ACADS, ACAT1, ACOX3, CPT1C, CPT2, ECHDC2, HADH, PPARGC1A* were differentially expressed (Figure 3b and 3c). Of these genes, the transcriptional coactivator PGC-1α (*PPARGC1A*) was virtually not expressed in hMVECs, while PGC-1α was highly upregulated in hiPSC-ECs (Figure 3d). This upregulation was confirmed with qPCR in hiPSC-EC batches originating from two different donors, indicating that despite the intrinsic heterogeneity of hiPSC-ECs the observed upregulation was not donor specific (Figure 3e). Systemic and cellular lipid metabolism is regulated by peroxisome proliferator-activated receptors (PPARs): PPARα, PPARβ/δ, and PPARγ. Among these isoforms, PPARγ is primarily a regulator of lipid storage and transport. PPARγ2 expression is mainly limited to adipose tissue,



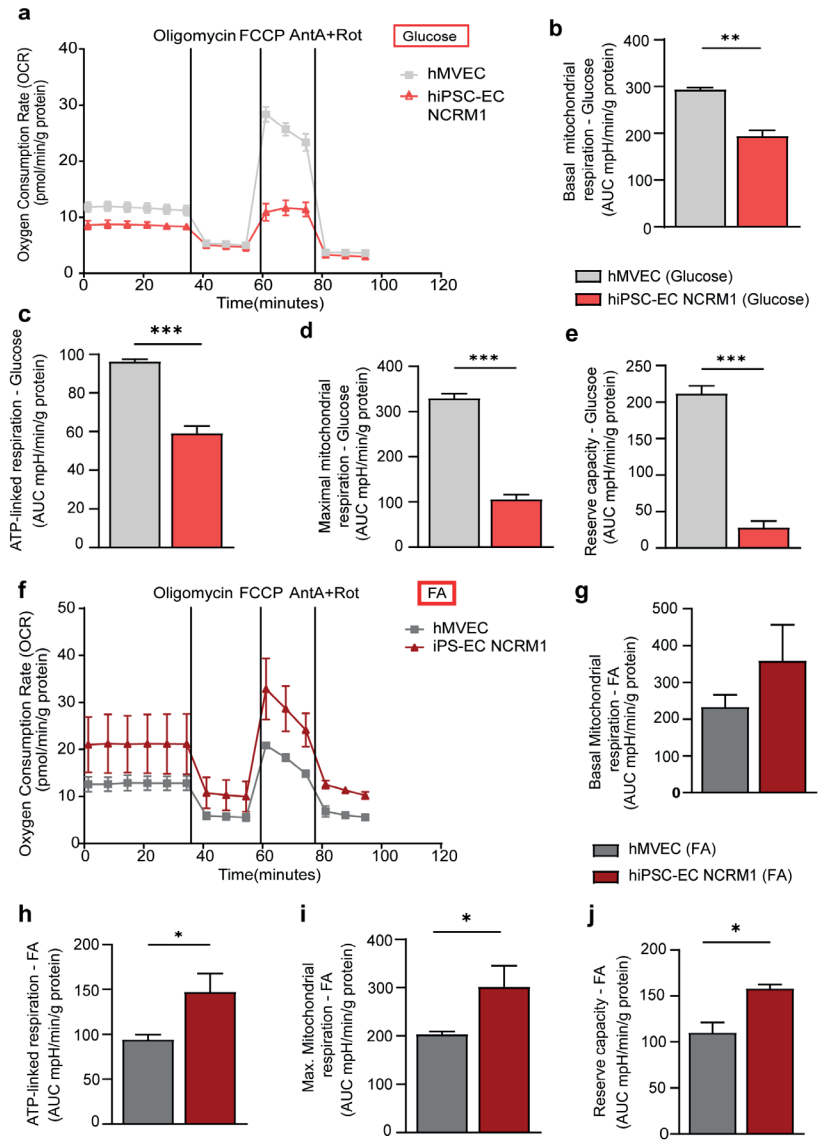


**Figure 1: hiPSC-ECs show a lower glucose-dependent oxidation, but a higher FAO compared to hMVECs.** Using a Seahorse XF Flux Analyzer **(a)** oxygen consumption rate (OCR) of hMVECs and hiPSC-ECs with glucose as energy substrate were measured. Basal mitochondrial respiration **(b)**, ATP-linked respiration **(c)**, maximal mitochondrial respiration **(d)** and the mitochondrial reserve capacity **(e)** of hMVECs and hiPSC-ECs with glucose as energy substrate are shown. **(f)** oxygen consumption rate (OCR) of hMVECs and hiPSC-ECs with palmitate as energy substrate were measured. Basal mitochondrial respiration **(g)**, ATP-linked respiration **(h)**, maximal mitochondrial respiration **(i)** and the mitochondrial reserve capacity **(j)** of hMVECs and hiPSC-ECs with palmitate as energy substrate are shown. Values are given as mean ± s.e.m. for the bar graphs and mean + s.d. for the OCR plot (N=4). Differences between cell types were assessed using an unpaired t test; *P ≤ 0.05, **P ≤ 0.01, ***P ≤ 0.001.

whereas PPARγ1 is expressed in various tissues including vascular ECs. Activation of PPARγ expression may be adaptive in order for the ECs to take up FAs vigorously to support ATP synthesis[24, 25,26].

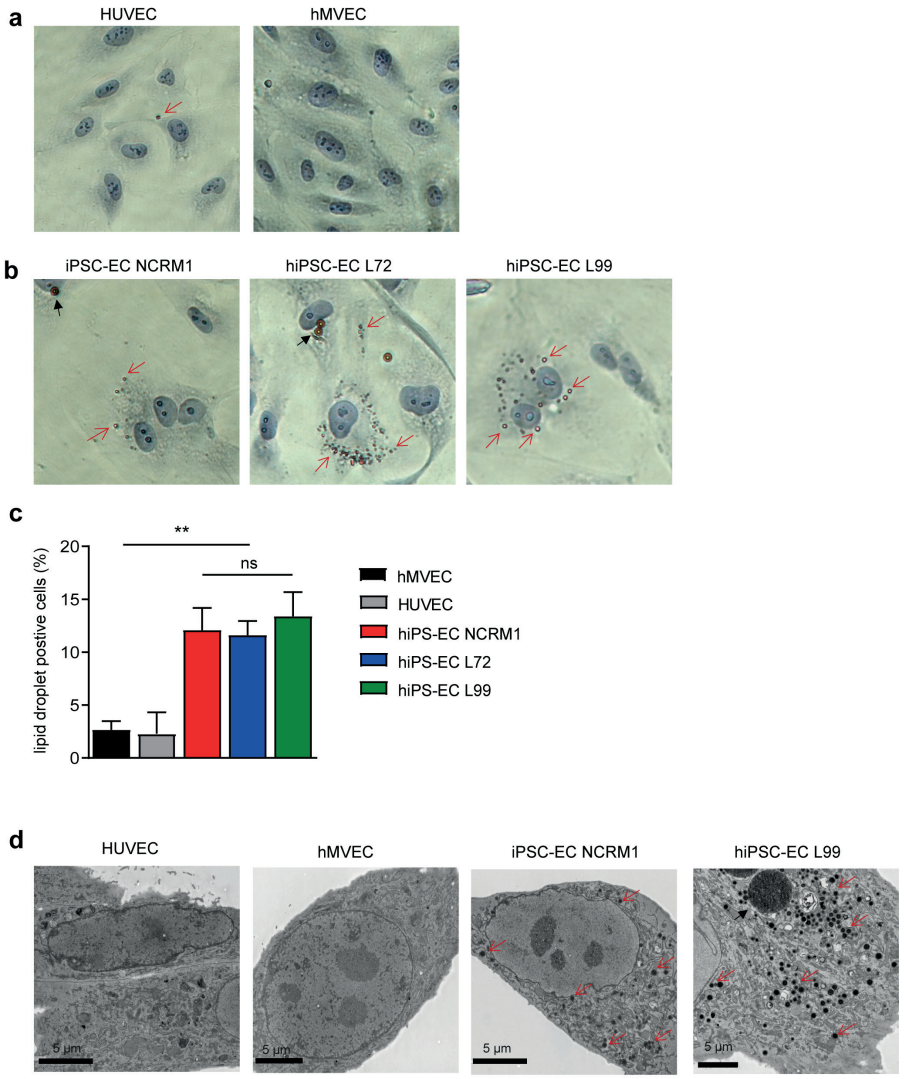


**Figure 2: Oil-red-O staining and TEM reveals increased amounts of lipid droplets in hiPSC-EC.** Representative brightfield images after staining with Oil-red-O of **(a)** primary EC; HUVEC and hMVEC and **(b)** hiPSC-EC derived from 3 IPSC lines NCMR1**,** LUMC72 and LUMC99. Red arrow indicates lipid droplet and black arrow CD31 magnetic bead. **(c)** Quantification of percentage of cells positive for oil-red-o staining. **(d)** Transmission Electron Microscopy (TEM) images reveal increased amounts of small lipid droplets (red arrow) in hiPSC-ECs compared to primary endothelial cells HUVEC and hMVEC**.** The black arrow indicates CD31 magnetic beads.



To substantiate these findings at the gene expression level, multiple subsequent attempts were focused on quantifying the PGC-1α protein level in hiPSC-ECs and hMVECs. Unfortunately, even using various antibodies for PGC-1α gave inconsistent results, as exemplified by Western blot (Supplementary Figure 2). To surpass this lack in proper quantification we pursued confirmation of the role of PGC-1α using downstream targets and functional assays for PGC1α.

## Blocking PGC-1α activity in hiPSC-ECs downregulates its genetic targets

As PGC-1α is known to play an important role in steering the cell's metabolism, we hypothesized that blocking PGC-1α expression in hiPSC-EC would lead to a metabolic switch from mainly FAO to a more glucose dependent metabolism.[27] Initially the specific PGC-1α inhibitor SR-18292 was used, which has no direct effect on gene and protein levels, but forces PGC-1α into an inactive form by acetylation. After a 2-day culture in the presence of SR-18292 (5 or 10 mM), RNA expression of PGC-1α was dose-dependently downregulated (Figure 4a). Gene expression measurements on downstream PGC-1α targets *PKM, TFAM, NOTCH1, PPARA, PPARB, NRF1* and *ESSRA*, however, did not provide conclusive results (data not shown). Therefore, two lentiviral vectors of the two most potent short hairpin RNAs sequences for PGC-1α (shPGC-1α) were constructed (Supplementary Figure 3a), achieving significant knock-down of PGC-1α expression in hiPSC-EC (Figure 4b). In hiPSC-EC, shPGC1α knockdown resulted also in reduction of its downstream targets (Supplementary Figure 3b-h). As expected, this downregulation indicated that the knock-down occurred not only at the gene expression level, but also at protein level.

## shRNA mediated knock-down of PGC-1α further increases FAO-dependent mitochondrial respiration

After lentiviral shPGC-1α transduction, hiPSC-ECs were again analysed using the Seahorse metabolic assay. In contrast to our expectations, the same rate of glycolysis with reduced glycolytic capacity and glycolytic reserve was found in shPGC-1α transduced hiPSC-EC as compared to mock transduction (Figure 5a-c). Also shPGC-1α hiPSC-ECs did not show a difference compared to mock hiPSC-ECs in mitochondrial function when provided with glucose as substrate for mitochondrial respiration (Figure 5d-h). The most striking result was that hiPSC-ECs transduced with shPGC-1α displayed an even higher fatty acid dependent respiration compared to the mock transduced cells, with a trend towards an increase of basal mitochondrial respiration and ATP-linked respiration and a significant elevation of maximal mitochondrial respiration and mitochondrial reserve capacity (Figure 6).

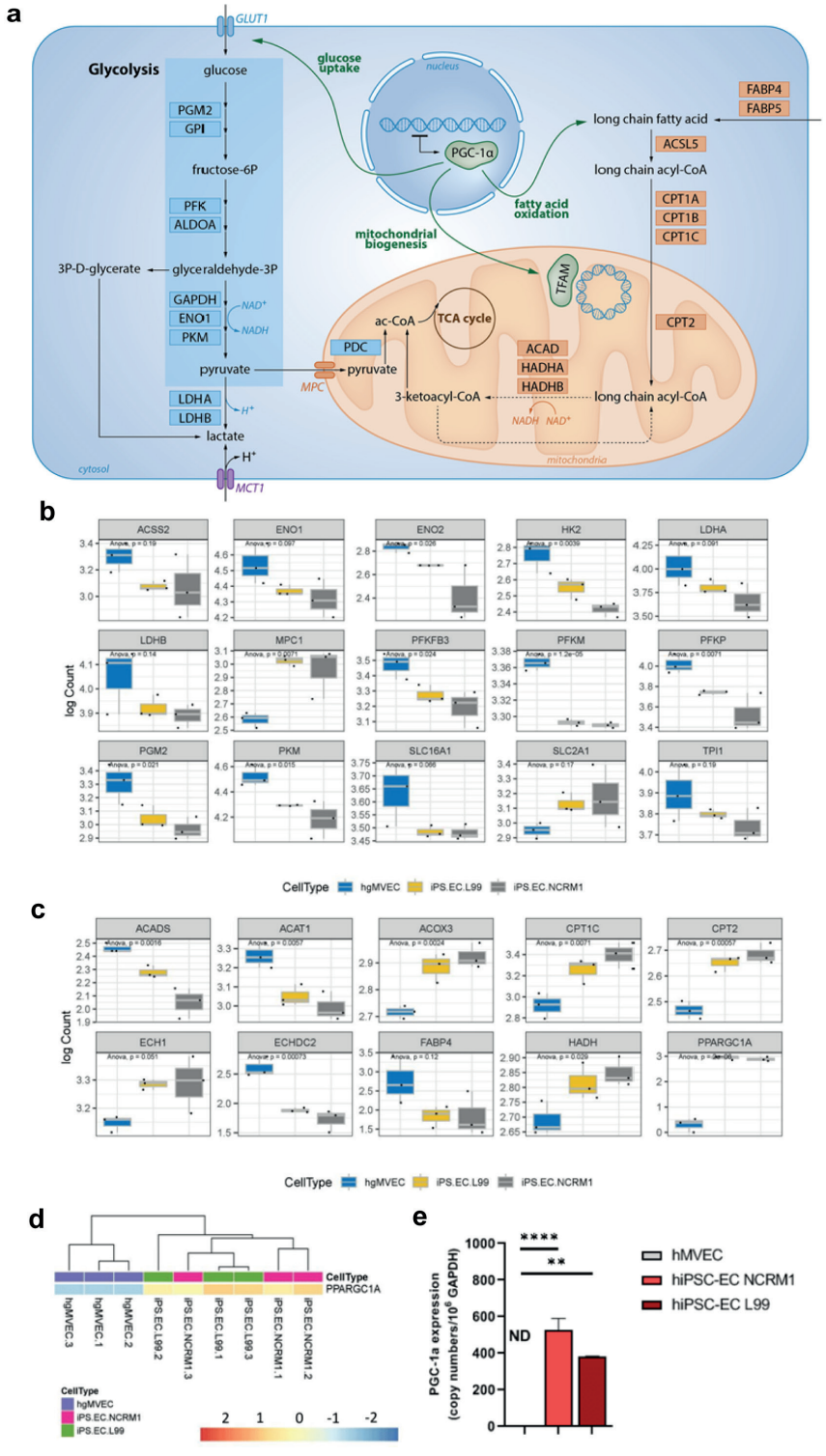




**Figure 3: PGC-1α expression is upregulated in hiPSC-ECs. (a)** Schematic overview of the most important pathways in endothelial cell metabolism. "DESeq2" package in R was used to generate the box plot of differentially expressed genes of glycolysis **(b)** and FAO metabolism **(c)** acquired from RNA-sequencing results. **(d)** Heatmap of PGC-1α from RNA-sequencing results. Experiments were performed after 4 days of cell culture of hMVECs, hiPSC-ECs NCRM1 and hiPSC-ECs L99. Red indicates upregulation and blue indicates downregulation of gene expression. **(e)** qPCR data of PGC-1α expression in hMVEC, hiPSC-EC NCRM1 (N=6) and hiPSC-EC L99 (N=2). Values are given as mean ± s.e.m. Differences between the cell types were assessed using an ordinary one-way ANOVA; **P ≤ 0.01, ****P < 0.0001.



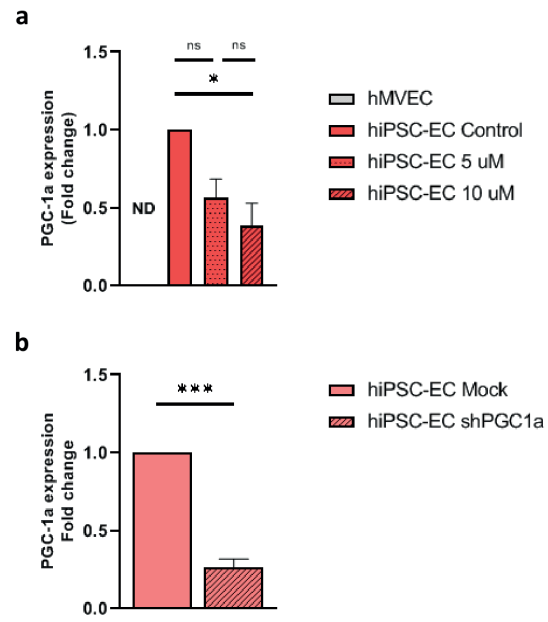


**Figure 4: Chemical and shRNA mediated knock-down of PGC-1α gene expression. (a)** qPCR data of PGC-1α expression in control hMVECs and hiPSC-ECs and in hiPSC-ECs cultured with 5 or 10 mM SR-18292. **(b)** qPCR data of PGC-1α expression in hiPSC-ECs transduced with mock and shPGC-1α. Values are given as mean ± s.e.m. Differences between cell types were assessed using an ordinary one-way ANOVA for the SR-18292 data and with an unpaired t test for the shRNA data; *P ≤ 0.05, **P ≤ 0.01, ***P ≤ 0.001

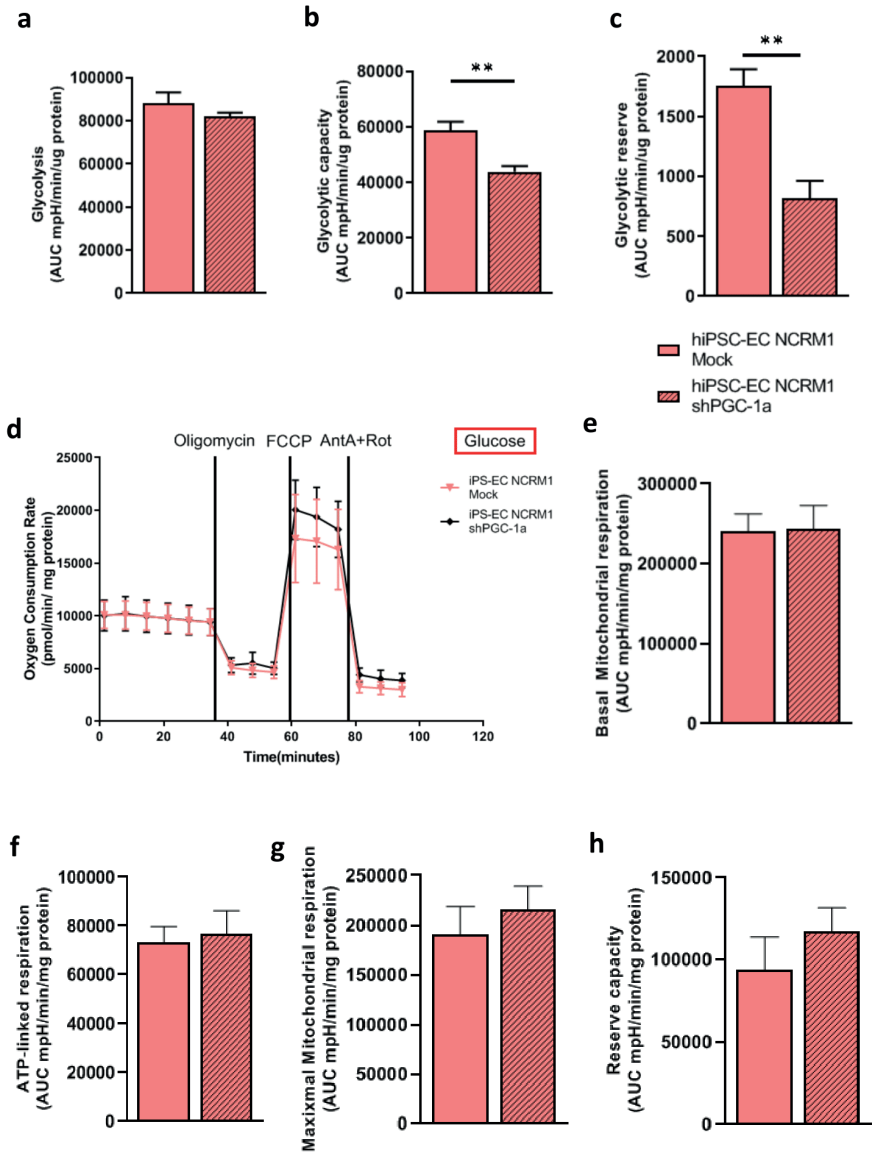


**Figure 5: Knockdown of PGC-1α in hiPSC-EC does not influence the glucose-dependent oxidation.** Using a Seahorse XF Flux Analyzer glycolysis **(a)**, glycolytic capacity **(b)** and the glycolytic reserve capacity **(c)** of hiPSC-ECs transduced with mock and shPGC-1α were measured. **(d)** The oxygen consumption rate (OCR) of hiPSC-ECs transduced with mock and shPGC-1α with glucose as energy substrate. Basal mitochondrial respiration **(e)**, ATP-linked respiration **(f)**, maximal mitochondrial respiration **(g)** and the mitochondrial reserve capacity of hiPSC-ECs transduced with mock and shPGC-1α with glucose as energy substrate. Values are given as mean ± s.e.m. for the bar graphs and mean + s.d. for the OCR plot (technical N=4). Differences between the cell types were assessed using unpaired t test; *P ≤ 0.05, **P ≤ 0.01



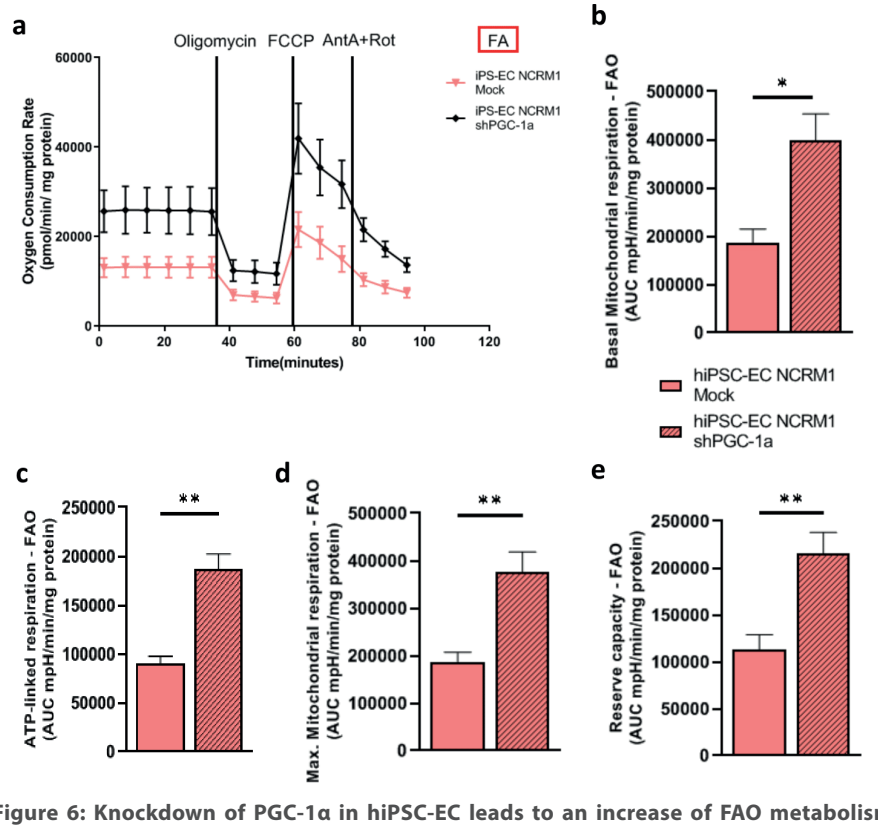


**Figure 6: Knockdown of PGC-1α in hiPSC-EC leads to an increase of FAO metabolism.** **(a)** Using a Seahorse XF Flux Analyzer the oxygen consumption rate (OCR) of hiPSC-ECs transduced with mock and shPGC-1α with palmitate as energy substrate were measured. Basal mitochondrial respiration **(b)**, ATP-linked respiration **(c)**, maximal mitochondrial respiration **(d)** and the mitochondrial reserve capacity **(e)** of hiPSC-ECs transduced with mock and shPGC-1α with palmitate as energy substrate. Values are given as mean ± s.e.m. for the bar graphs and mean + s.d. for the OCR plot (technical N=4). Differences between the cell types were assessed using an unpaired t test; *P ≤ 0.05.

## Discussion

These results reveal that the metabolism of hiPSC-ECs is remarkably distinct from that of primary hMVECs, especially with respect to their fuel used for mitochondrial respiration. Where hMVECs mainly rely on glucose-dependent mitochondrial respiration, hiPSC-ECs seem to use this to a lesser extent and dominantly rely on fatty acid-dependent respiration. Under normal conditions, primary endothelial cells are known to be glycolysis-addicted for energy production and the cells die when deprived of glucose.[28] FAO normally does not contribute markedly to the energy

balance of ECs, as only 5% of the total amount of ATP formed comes from this part of metabolism.[29] However, FAO has a function in sustaining the TCA cycle and thereby providing enough substrate for deoxynucleotide triphosphate (dNTP) synthesis for proliferation and maintenance of ECs.[30]

In the present study, an attempt was made to direct the hiPSC-EC metabolism towards a more glucose-dependent metabolism by targeting the transcriptional coactivator PGC-1α, a well-known regulator of metabolism.[27,31-33] Through its influence on implicated transcription factors, PGC-1α affects key metabolic processes like mitochondrial biogenesis, glucose utilization, antioxidant detoxification and fatty acid oxidation. Furthermore, dysregulation of PGC-1α expression seems to be involved in cancer metabolism, neurodegenerative disorders, diabetes and kidney disease, which emphasizes the need for its proper regulation.[34-39] As PGC-1α is under normal conditions not expressed in hMVEC, we hypothesized that reducing its expression in hiPSC-EC might normalize the hiPSC-EC metabolism. Contrary to our expectations, PGC-1α knock-down resulted in an even higher elevation of fatty acid metabolism in hiPSC-EC without affecting glucose metabolism. This observation implies that the dependency on FAO metabolism is not caused by the upregulation of PGC-1α and there seems to be another role for FAO metabolism in hiPSC-EC. This role of PGC1α might be to sustain the TCA cycle by supplying acetyl-CoA and thereby enabling the regeneration of NADPH from $NADP^+$ in order to maintain the redox balance of the cell, as is the case in quiescent ECs.[15] The observed reduced amounts of glutathione, the main ROS scavenger, could also be an additional driver of this alternative redox balancing system. Redox homeostasis is particularly important, since hiPSC-EC previously showed higher reactive oxygen species levels [40], affecting the intracellular redox state.[41]

Furthermore, since glycolysis levels are significant lower in hiPSC-ECs compared to hMVECs, as described before [19], it seems that hiPSC-EC are unable to provide glycolytic metabolites as substrate for mitochondrial respiration. The glycolytic flux to both lactate and pyruvate is lower, [19] however, similar levels of ATP production were found, indicating that the hiPSC-ECs use another metabolite to provide enough substrate for the TCA cycle, such as FFA which is a potent alternative acetyl-CoA source, contributing to the fatty acid-dependent metabolism in hiPSC-ECs.[40]

It should be noted, that PGC-1α is not the only transcriptional co-activator and that additional targets are identified in literature. The nuclear receptor co-activators and repressors (NCoA and NCoR) and histone deacetylases (HDAC) have been implicated in mitochondrial respiration and FAO metabolism and, although we did not observe significant differences at the transcriptional level, they could potentially replace the role of PGC-1α or play their own role in affecting hiPSC-EC metabolism.[42] Moreover, upstream signaling pathways which modulate the activity of these co-regulators, for example AMP-activated protein kinase (AMPK) signaling pathway is reported to affect mitochondrial biogenesis, redox homeostasis, glucose metabolism and FAO metabolism. [43,44,45]

Our recent studies reveal that the immaturity of hiPSC-EC is characterized by an altered cellular metabolism. The reduced glycolysis results in a increased intracellular pH affecting the formation of Weibel Palade Bodies, a main functional body of all EC.[19] Furthermore, the increased ROS, caused by leaking immature mitochondria and the reliance on FFO, damages the glycocalyx and reduces the functionality of the cells.[46] Although influencing one aspect of the metabolism, such as closure of the mitochondrial transition pore, resulting in several improved aspects of the cell, it did not alter the internal pH and therefore did not result in maturation of Weibel Palade Bodies in hiPSC-ECs. Therefore we argue that we lack fundamental knowledge on the role of metabolism in human development and the metabolic processes involved in maturation. To generate mature and functional cells and tissues from IPSC we have to gain more insight into the metabolic processes driving differentiation, maturation and (epi)genetic modulation.

## References


1 Tewary, M., Shakiba, N. & Zandstra, P. W. Stem cell bioengineering: building from stem cell biology. *Nat Rev Genet* **19**, 595-614, doi:10.1038/s41576-018-0040-z (2018).
2 Fisher, M. B. & Mauck, R. L. Tissue engineering and regenerative medicine: recent innovations and the transition to translation. *Tissue Eng Part B Rev* **19**, 1-13, doi:10.1089/ten.TEB.2012.0723 (2013).
3 Mao, A. S. & Mooney, D. J. Regenerative medicine: Current therapies and future directions. *Proc Natl Acad Sci U S A* **112**, 14452-14459, doi:10.1073/pnas.1508520112 (2015).
4 Buckler, L. Opportunities in regenerative medicine. *BioProcess International*, 14-18 (2011).
5 Takahashi, K. & Yamanaka, S. Induction of pluripotent stem cells from mouse embryonic and adult fibroblast cultures by defined factors. *Cell* **126**, 663-676, doi:10.1016/j.cell.2006.07.024 (2006).
6 Takahashi, K. *et al.* Induction of pluripotent stem cells from adult human fibroblasts by defined factors. *Cell* **131**, 861-872, doi:10.1016/j.cell.2007.11.019 (2007).
7 Yu, J. *et al.* Induced Pluripotent Stem Cell Lines Derived from Human Somatic Cells. *Science* **318**, 1917-1920 (2007).
8 Kaji, K. *et al.* Virus-free induction of pluripotency and subsequent excision of reprogramming factors. *Nature* **458**, 771-775, doi:10.1038/nature07864 (2009).
9 Woltjen, K. *et al.* piggyBac transposition reprograms fibroblasts to induced pluripotent stem cells. *Nature* **458**, 766-770, doi:10.1038/nature07863 (2009).
10 Dai, Z. & Locasale, J. W. Understanding metabolism with flux analysis: From theory to application. *Metabolic Engineering* **43**, 94-102, doi:10.1016/j.ymben.2016.09.005 (2017).
11 Patti, G. J., Yanes, O. & Siuzdak, G. Metabolomics: the apogee of the omics trilogy. *Nat Rev Mol Cell Biol* **13**, 263-269, doi:10.1038/nrm3314 (2012).
12 Eelen, G. *et al.* Endothelial Cell Metabolism. *Physiological Reviews* **98**, 3-58, doi:10.1152/physrev.00001.2017 (2018).
13 Rohlenova, K., Veys, K., Miranda-Santos, I., De Bock, K. & Carmeliet, P. Endothelial Cell Metabolism in Health and Disease. *Trends in Cell Biology* **28**, 224-236, doi:10.1016/j.tcb.2017.10.010 (2018).
14 Carmeliet, P. **Angiogenesis in health and disease**. *Nature Medicine* **9**, 653-660 (2003).
15 Kalucka, J. *et al.* Quiescent Endothelial Cells Upregulate Fatty Acid beta-Oxidation for Vasculoprotection via Redox Homeostasis. *Cell metabolism* **28**, 881-894.e813, doi:10.1016/j.cmet.2018.07.016 (2018).
16 Kosmides, A. K., Kamisoglu, K., Calvano, S. E., Corbett, S. A. & Androulakis, I. P. Metabolomic Fingerprinting: Challenges and Opportunities. *Crit Rev Biomed Eng* **41**, 205-221 (2013).
17 Orlova, V. V. *et al.* Generation, expansion and functional analysis of endothelial cells and pericytes derived from human pluripotent stem cells. *Nature Protocols* **9**, 1514-1531, doi:10.1038/nprot.2014.102 (2014).
18 Divakaruni, A. S., Paradyse, A., Ferrick, D. A., Murphy, A. N. & Jastroch, M. in *Mitochondrial Function Methods in Enzymology* 309-354 (2014).
19 Tiemeier, G. L. *et al.* Lowering the increased intracellular pH of human-induced pluripotent stem cell-derived endothelial cells induces formation of mature Weibel-Palade bodies. *STEM CELLS Translational Medicine* **n/a**, doi:10.1002/sctm.19-0392.
20 Kuo, A., Lee Monica, Y. & Sessa William, C. Lipid Droplet Biogenesis and Function in the Endothelium. *Circulation Research* **120**, 1289-1297, doi:10.1161/CIRCRESAHA.116.310498 (2017).
21 Heid, H. *et al.* On the formation of lipid droplets in human adipocytes: the organization of the perilipin-vimentin cortex. *PloS one* **9**, e90386-e90386, doi:10.1371/journal.pone.0090386 (2014).
22 Yang, H., Galea, A., Sytnyk, V. & Crossley, M. Controlling the size of lipid droplets: lipid and protein factors. *Current Opinion in Cell Biology* **24**, 509-516, doi:https://doi.org/10.1016/j.ceb.2012.05.012 (2012).
23 Kuo, A., Lee, M. Y. & Sessa, W. C. Lipid Droplet Biogenesis and Function in the Endothelium. *Circulation Research* **120**, 1289-1297, doi:doi:10.1161/CIRCRESAHA.116.310498 (2017).
24 Goto, K. *et al.* Peroxisome Proliferator-Activated Receptor-γ in Capillary Endothelia Promotes Fatty Acid Uptake by Heart During Long-Term Fasting. *Journal of the American Heart Association* **2**, e004861, doi:10.1161/JAHA.112.004861.
25 Duan Sheng, Z., Usher Michael, G. & Mortensen Richard, M. Peroxisome Proliferator-Activated Receptor-γ–Mediated Effects in the Vasculature. *Circulation Research* **102**, 283-294, doi:10.1161/CIRCRESAHA.107.164384 (2008).
26 Vidal-Puig, A. J. *et al.* Peroxisome proliferator-activated receptor gene expression in human tissues. Effects of obesity, weight loss, and regulation by insulin and glucocorticoids. *The Journal of Clinical Investigation* **99**, 2416-2422, doi:10.1172/JCI119424 (1997).
27 Lin, J., Handschin, C. & Spiegelman, B. M. Metabolic control through the PGC-1 family of transcription coactivators. *Cell Metab* **1**, 361-370, doi:10.1016/j.cmet.2005.05.004 (2005).
28 Draoui, N., de Zeeuw, P. & Carmeliet, P. Angiogenesis revisited from a metabolic perspective: role and therapeutic implications of endothelial cell metabolism. *Open Biol* **7**, doi:10.1098/rsob.170219 (2017).
29 De Bock, K. *et al.* Role of PFKFB3-driven glycolysis in vessel sprouting. *Cell* **154**, 651-663, doi:10.1016/j.cell.2013.06.037 (2013).
30 Schoors, S. *et al.* Fatty acid carbon is essential for dNTP synthesis in endothelial cells. *Nature* **520**, 192-197, doi:10.1038/nature14362 (2015).
31 Fernandez-Marcos, P. J. & Auwerx, J. Regulation of PGC-1alpha, a nodal regulator of mitochondrial biogenesis. *Am J Clin Nutr* **93**, 884S-890, doi:10.3945/ajcn.110.001917 (2011).
32 Puigserver, P. & Spiegelman, B. M. Peroxisome proliferator-activated receptor-gamma coactivator 1 alpha (PGC-1 alpha): transcriptional coactivator and metabolic regulator. *Endocr Rev* **24**, 78-90, doi:10.1210/er.2002-0012 (2003).
33 Finck, B. N. & Kelly, D. P. PGC-1 coactivators: inducible regulators of energy metabolism in health and disease. *The Journal of Clinical Investigation* **116**, 615-622, doi:10.1172/JCI27794 (2006).
34 Mastropasqua, F., Girolimetti, G. & Shoshan, M. PGC1alpha: Friend or Foe in Cancer? *Genes (Basel)* **9**, doi:10.3390/genes9010048 (2018).
35 Tan, Z. *et al.* The Role of PGC1alpha in Cancer Metabolism and its Therapeutic Implications. *Mol Cancer Ther* **15**, 774-782, doi:10.1158/1535-7163.MCT-15-0621 (2016).
36 Austin, S. & St-Pierre, J. PGC1alpha and mitochondrial metabolism--emerging concepts and relevance in ageing and neurodegenerative disorders. *J Cell Sci* **125**, 4963-4971, doi:10.1242/jcs.113662 (2012).
37 Sawada, N. *et al.* Endothelial PGC-1alpha mediates vascular dysfunction in diabetes. *Cell Metab* **19**, 246-258, doi:10.1016/j.cmet.2013.12.014 (2014).
38 Lynch, M. R., Tran, M. T. & Parikh, S. M. PGC1alpha in the kidney. *Am J Physiol Renal Physiol* **314**, F1-F8, doi:10.1152/ajprenal.00263.2017 (2018).
39 Han, S. H. *et al.* PGC-1alpha Protects from Notch-Induced Kidney Fibrosis Development. *J Am Soc Nephrol* **28**, 3312-3322, doi:10.1681/ASN.2017020130 (2017).
40 Tiemeier, G. L. *et al.* Closing the Mitochondrial Permeability Transition Pore in hiPSC-Derived Endothelial Cells Induces Glycocalyx Formation and Functional Maturation. *Stem Cell Reports* **13**, 803-816, doi:10.1016/j.stemcr.2019.10.005 (2019).
41 He, L. *et al.* Antioxidants Maintain Cellular Redox Homeostasis by Elimination of Reactive Oxygen Species. *Cell Physiol Biochem* **44**, 532-553, doi:10.1159/000485089 (2017).
42 Mouchiroud, L., Eichner, L. J., Shaw, R. J. & Auwerx, J. Transcriptional coregulators: fine-tuning metabolism. *Cell Metab* **20**, 26-40, doi:10.1016/j.cmet.2014.03.027 (2014).
43 Mihaylova, M. M. & Shaw, R. J. The AMPK signalling pathway coordinates cell growth, autophagy and metabolism. *Nat Cell Biol* **13**, 1016-1023, doi:10.1038/ncb2329 (2011).
44 Fisslthaler, B. & Fleming, I. Activation and Signaling by the AMP-Activated Protein Kinase in Endothelial Cells. *Circulation Research* **105**, 114-127, doi:10.1161/circresaha.109.201590 (2009).

45 Jornayvaz, F. R. & Shulman, G. I. Regulation of mitochondrial biogenesis. *Essays Biochem* **47**, 69-84, doi:10.1042/bse0470069 (2010).
46 Gesa L. Tiemeier, G. W., Sébastien J. Dumas, Wendy M.P.J. Sol, M. Cristina Avramut, Tobias Karakach, Valeria V. Orlova, Cathelijne W. van den Berg, Christine L. Mummery, Peter Carmeliet, Bernard M. van den Berg, Ton J. Rabelink. Closing the Mitochondrial Permeability Transition Pore in hiPSC-Derived Endothelial Cells Induces Glyococalyx Formation and Functional Maturation. *Stem Cell Reports* **Vol.1 13**, 1-14 (2019).
47 Lambrechts, D. *et al.* Phenotype molding of stromal cells in the lung tumor microenvironment. *Nat Med* **24**, 1277-1289, doi:10.1038/s41591-018-0096-5 (2018).
48 Kostidis, S., Addie, R. D., Morreau, H., Mayboroda, O. A. & Giera, M. Quantitative NMR analysis of intra- and extracellular metabolism of mammalian cells: A tutorial. *Analytica Chimica Acta* **980**, 1-24 (2017).
49 Vinaixa, M. *et al.* Positional Enrichment by Proton Analysis (PEPA): A One-Dimensional 1H-NMR Approach for 13C Stable Isotope Tracer Studies in Metabolomics. *Angewandte Chemie International Edition* **56**, 3531-3535, doi:10.1002/anie.201611347 (2017).



## Supplementary Figures

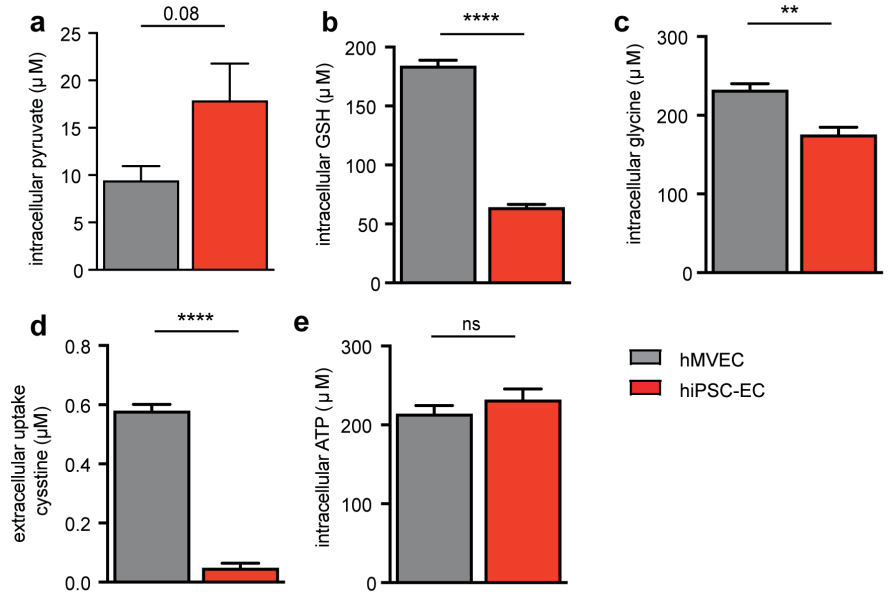


**Supplementary Figure 1: hiPSC-EC have reduced production of intracellular antioxidants.** Nuclear magnetic resonance (NMR) spectroscopy was used to determine the cellular metabolites**: (a)** Total intracellular pyruvate concentrations **(b)** total intracellular GSH concentrations **(c)** total intracellular glycine concentrations **(d)** total extracellular cystine concentrations **(e)** total intracellular ATP concentrations. Values are given as mean ± s.e.m. Differences between the cell types were assessed using an unpaired t test; *P ≤ 0.05, **P ≤ 0.01, **** P≤ 0.0001, ns = non-significant.

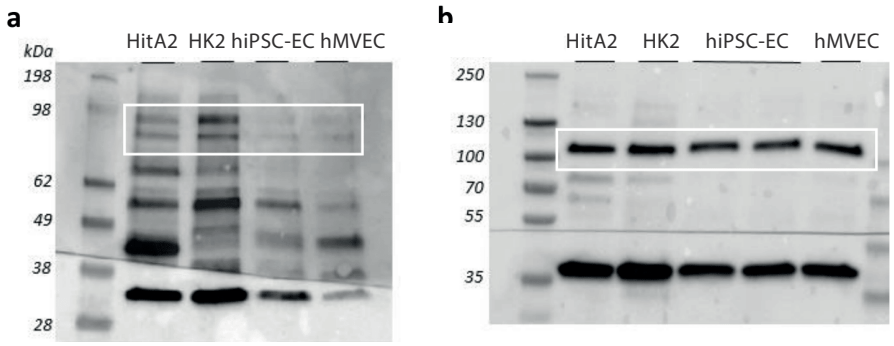


**Supplementary Figure 2: Western blot analyses of PGC-1α showed inconsistent results using different antibodies. (a)** Western blot analysis of PGC-1α protein expression in Human Internal thoracic A2 cells (HitA2), Human Kidney cells (HK2), hiPSC-EC NCRM1 (iPS-EC) and hMVEC (GENC) using the Invitrogen antibody and the SeeBlue Plus2 Pre-stained protein ladder. **(b)** Western blot analysis of PGC-1α protein expression in HitA2, HK2, iPS-EC and GENC using the Novus Biologicals antibody and the PageRuler Plus Prestained protein ladder.





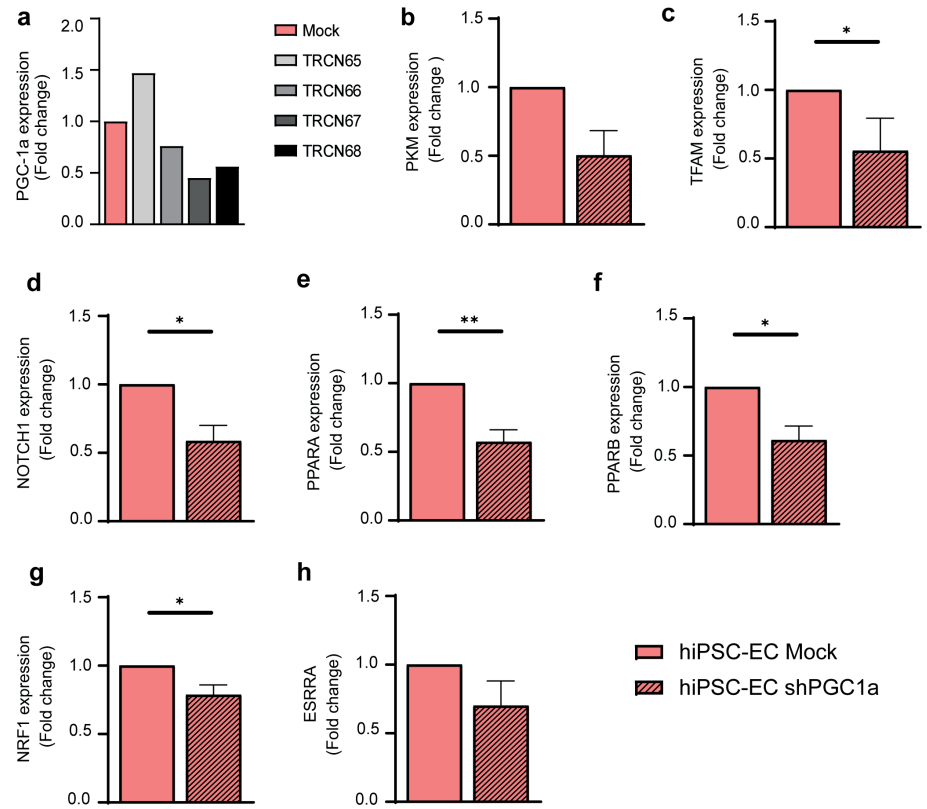


**Supplementary Figure 3: Genetic knock-down of PGC-1α leads to a reduction in gene expression of its downstream targets.** qPCR data of **(a)** PGC-1α expression after lentiviral treatment with mock and the TRCN0000001165, TRCN0000001166, TRCN0000001167, TRCN0000001168 shRNA vectors. *PKM* **(b)**, *TFAM* **(c)**, *NOTCH1* **(d)**, *PPARA* **(e)**, *PPARB* **(f)**, *NRF1* **(g)** and *ESRRA* **(h)** expression in hiPSC-ECs transduced with mock and shPGC-1α (N=3). Values are given as mean ± s.e.m. Differences between the cell types were assessed using an unpaired t test; *P ≤ 0.05, **P ≤ 0.01.